Supporting Information

A Comprehensive Model of Electric-Field-Enhanced Jumping-Droplet Condensation on Superhydrophobic Surfaces

Patrick Birbarah, Zhaoer Li, Alexander Pauls, Nenad Miljkovic*

Department of Mechanical Science and Engineering, University of Illinois, Urbana, Illinois 61801, United States

*Address correspondence to nmiljkov@illinois.edu.

S.1 MOVIES

Movie 1. Experimental high speed video (captured by Phantom v7.1, Vision Research camera) showing a droplet of radius 14 μm jumping upward from a SPF coated horizontal superhydrophobic surface. The video is captured at a rate of 2900 fps and played back at 20 fps. The size of the image is 800x600 pixels, which represents 3.5x2.6 mm. For surface fabrication and functionalization details, please see references 32.

Movie 2. Simulated trajectory of a 14 μm radius droplet jumping upward from a SPF coated horizontal superhydrophobic surface. The initial velocity of the droplet considered was measured from Movie 1 *via* MATLAB and used in the MATLAB simulation ($u_{d,x}\big|_{t=0}$ = -0.08 m/s and $u_{d,y}\big|_{t=0}$ = 0.14 m/s). The video is played at 20 fps. The image represents 5.2 mm in the horizontal direction and 3.5 mm in the vertical direction.

S.2 Electrowetting on dielectric (EWOD) model

The EWOD model[1] predicts that the contact angle of a droplet would be altered if the droplet is subjected to an electric field, by the following formula:

$$\cos \theta' = \cos \theta + \frac{\epsilon_0 \epsilon_d}{2 d \sigma_{lv}} V^2, \tag{S1}$$

where θ' and θ represent the effective and the initial contact angles, respectively, $\epsilon_0 = 8.854 \times 10^{-12}$ F/m represents the permittivity of free space, ϵ_d represents the dielectric constant of the insulator ($\epsilon_d \approx 1$ for water vapor), d represents the thickness of the dielectric ($\approx$ electrode spacing s), σ_{lv} represents the liquid-vapor surface tension (72 mJ/m^2 for water-air), and V represents the applied voltage.

Figure S1 shows θ' for a range of voltages (300 – 1200 V) and spacings (1 - 100 mm) assuming an initial apparent advancing contact angle of 180°. The effective contact angle after the application of voltage was not lower than 170° for $s > 1$ cm. Hence, the effect of the change of surface tension (and subsequently of initial velocity of droplets) was deemed negligible and not considered in our EFE model. However, these effects need to be considered for cases having very small spacings (< 1mm) and high voltages (> 1000V).
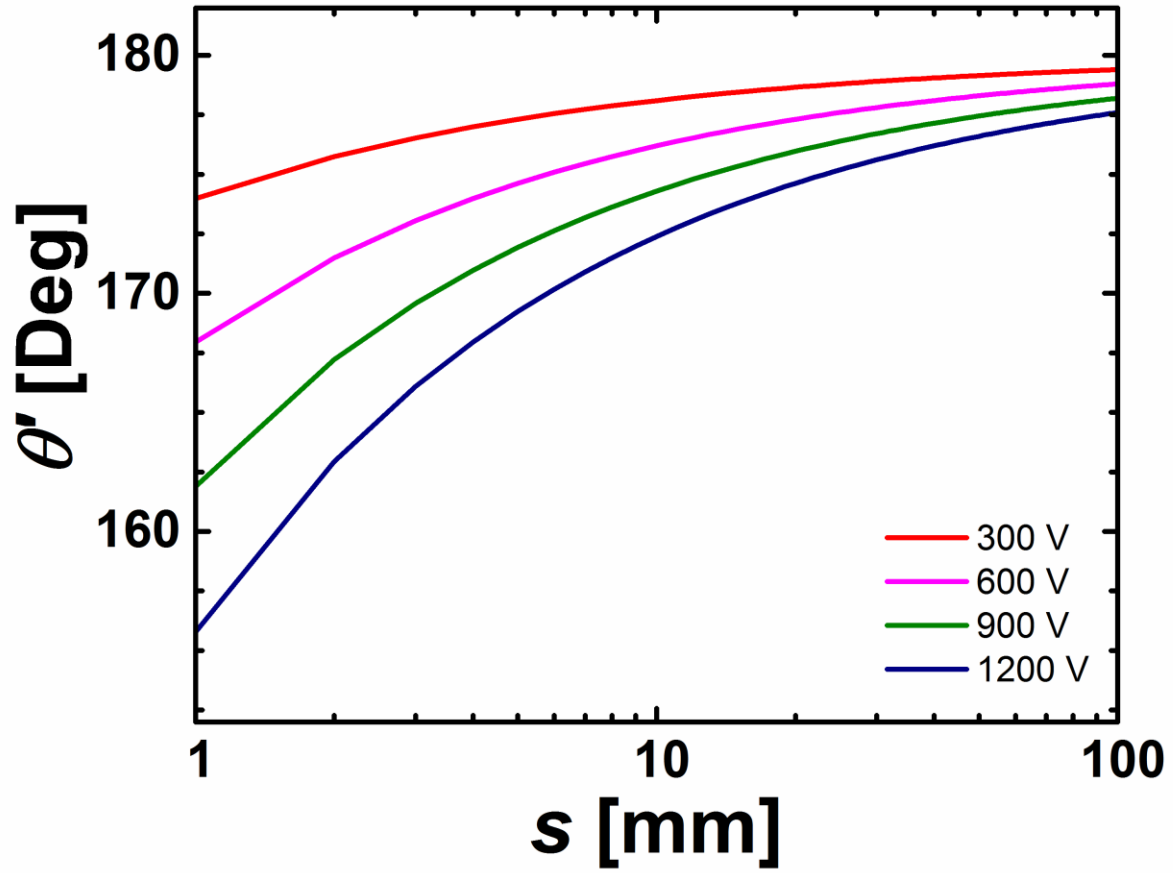
Figure S1. Effective contact angle (θ') due to applied voltage between the superhydrophobic condensing surface and an external electrode. The initial contact angle is assumed to be 180°. The effect of electrode spacing (s = 1-100 mm) and applied voltage (V = 300-1200 V) are calculated using Eq. (S1). For s > 1 cm no relevant change in contact angle is predicted (θ' > 170°).

S.3 Droplet Acceleration Analysis

In this section we propose a complementary explanation (other than the scaling analysis provided in the manuscript) for the behavior observed in Fig. 4a of the manuscript. The analysis is based on the variation of the acceleration, which is a droplet size-independent indicator of motion.

Dividing Eq. (7) of the manuscript by $(4/3)\pi R_d{}^3 \rho_w$, we obtain:

$$a_{d,y} = kR_d{}^{-1} - g + \frac{q_d E_y}{m}, \tag{S2}$$

where k is a factor combining all radius independent properties $(k = -3\rho_v C_D sgn(u_{d,x} + u_{v,x})(u_{d,y} + u_{v,y})^2/8\rho_w)$. From Eq. (S2) we can see that in the high radius limit $(R_d > 7$ μm, $q_d \sim R_d{}^2)$, both the electrostatic term and the drag force term decay which leaves only the gravitational term to overcome, hence V_{crit} increases. In this limit, in order to keep the same acceleration as we increase the droplet size, the electric field should increase linearly with R_d so that the rightmost term in Eq. (S2) becomes independent of R_d. This implies that the critical voltage should increase linearly since it is the only external control variable. However, in the low radius limit, where $q_d \sim$ constant, the electrostatic term dominates $(R_d{}^3$ dependence in the denominator) hence a large voltage in not needed to attract the droplet to the outer electrode. To better understand the region bridging the two limits, we plotted the acceleration in terms of the droplet radius (Eq. (S2)) for the parallel plate case using the numerical parameters of the initial problem (Fig. S2). Figure S2 exhibits a behavior opposite to the one observed in Fig. 4a, which is logical since lower acceleration implies higher voltage needed to remove it. Figure S2 shows

that the acceleration has a locally minimum at $R_d \approx 8$ μm, due to the complex balance of non-linear forces acting on the droplet in the electric field. A local minimum in acceleration with a negative phase indicates that the droplets are being rapidly decelerated on their trajectory to the outer electrode, meaning that a large electric filed or applied voltage must be used to fully remove them. This is in agreement with our results of Fig. 4a.
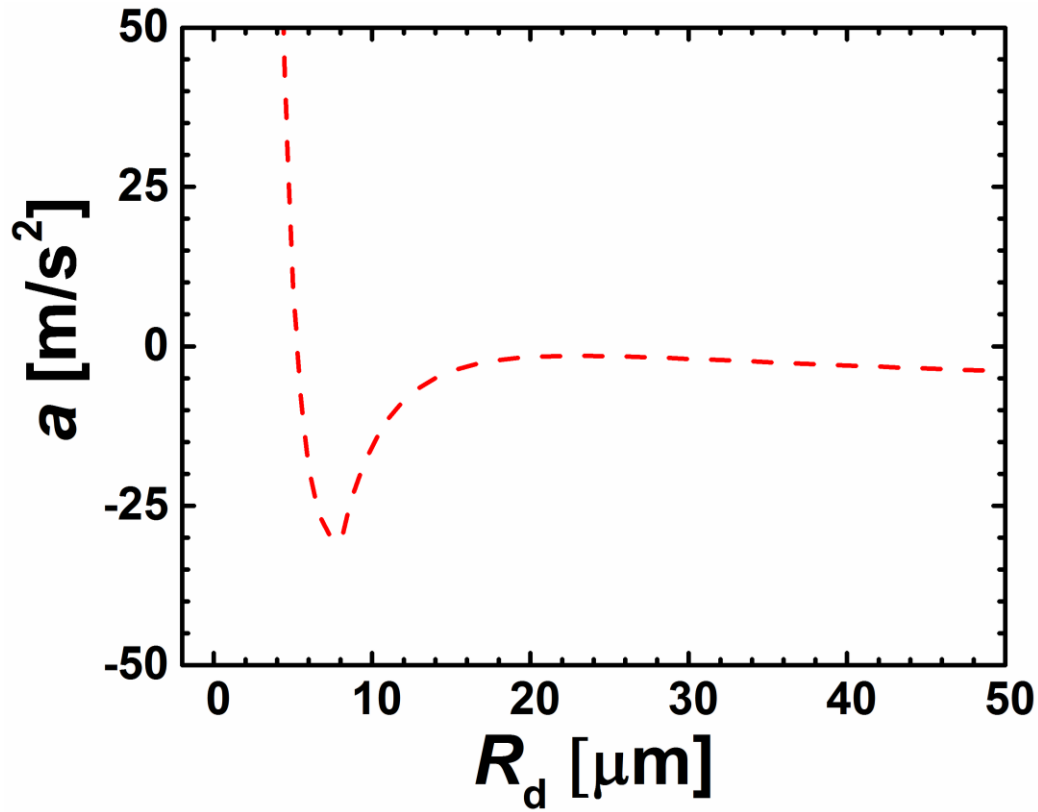

Figure S2. Upward acceleration (a) of a droplet of radius R_d jumping from a superhydrophobic SPF coated flat plate and subjected to an uniform external electric field $E = 75$ V/cm. The acceleration is found from Newton's second law applied on the droplet experiencing upward electrostatic force and downward drag and gravitational forces. The heat flux and relative vapor flow velocity are considered constant at 0.9 W/cm^2 and 0.2 m/s, respectively. The choice of velocity was aimed to represent the droplet at an intermediate position (0.2 m/s < 0.6 m/s which

is the initial relative velocity). The curve gives an explanation for the parallel case behavior observed in Fig. 5a, which can be generalized to both the cylindrical and spherical cases.

S.4 Large Radius Limit of Inner Condensing Electrode

In this section, we validate the consistency of the dependency of the electric field magnitude on the geometry of the electrodes by showing that for a large inner radius of the electrode, all geometries (parallel, cylindrical and spherical) reduce to the parallel plate case (Fig. S3).
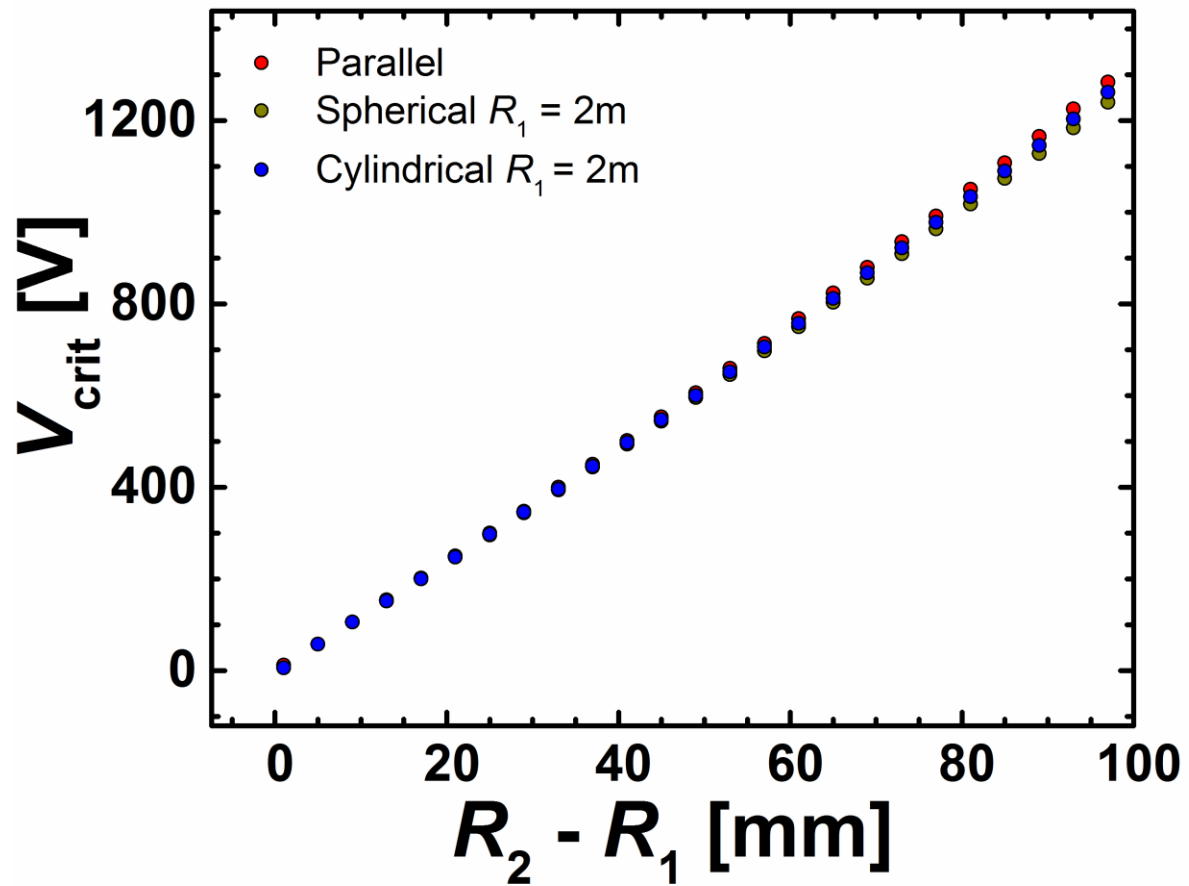
Figure S3. Convergence of the spherical and cylindrical geometries to the parallel plate in the large inner radius (R_1) limit. The critical voltage for droplet removal (V_{crit}) is shown for the three cases in terms of the spacing between the inner and outer electrode (radius R_2). The droplet considered has a 10 μm radius and the heat flux used in the simulation is 0.5 W/cm^2.

S.5 Matlab Code

Eight Matlab files have been appended to the supplementary materials section. Brief descriptions of the programs and what they accomplish are listed below:

1) '**DropletODE_P.m**': This code contains the system of differential equations governing the motion of a droplet jumping from a flat surface at an set inclination and subjected to an electric field established between two charged parallel plates.

2) '**DropletODE_C.m**': This code contains the system of differential equations governing the motion of a droplet jumping from a cylindrical or spherical surface, also subjected to an electric field established between two charged concentric surfaces, either cylindrical or spherical.

3) '**Initial_Condition_P.m**': This code sets the initial conditions of the droplet (position and velocity) for the parallel plate jumping case. The initial position depends on the inclination of the plates, while the initial velocity is given by an experimental correlation.

4) '**Plotting_parallel_plates.m**': This code plots the parallel plates for any inclination in order to be visually descriptive of the real droplet trajectory.

5) '**main_droplet_P.m**': This code is used to combine the subroutines 'DropletODE_P.m', 'Initial_Condition_P.m', and 'Plotting_parallel_plates.m' in order to solve and plot the results of the dynamic trajectory of a droplet jumping within a parallel plate capacitor.

6) '**main_droplet_C.m**': This code uses the function 'DropletODE_C.m' to solve for the dynamic trajectory of a droplet jumping from a spherical or cylindrical surface subjected to an electric field, and plots the resulting trajectory along with the concentric electrodes.

7) '**Trajectories_validation.m**': This code is used to compare the simulated trajectories to experimental videos in space and time, for the case of droplets jumping upward from a flat surface with no electric field applied.

8) '**EffectsOfParameters.m**': This code is used to vary different parameters of our system such as droplet size, heat flux, orientation of jumping, and geometry of electrodes, and generates the data that is used for the graphs present in our manuscript.

References

1.   Mugele, F.; Baret, J. C. Electrowetting: From basics to applications. *J Phys-Condens Mat* 2005, 17, R705-R774.